Nanometer size effect on magnetic order in $La_{0.4}Ca_{0.6}MnO_3$: Predominant influence of doped electron localization

E. Rozenberg,[1,*] M. Auslender,[1] A. I. Shames,[1] D. Mogilyansky,[1] I. Felner,[2] E. Sominskii,[3] A. Gedanken,[3] and Ya. M. Mukovskii[4]

[1]*Department of Physics, Ben-Gurion University of the Negev, P.O. Box 653, Beer-Sheva 84105, Israel*

[2]*The Racah Institute of Physics, The Hebrew University, Jerusalem 91904, Israel*

[3]*Department of Chemistry and Kanbar Laboratory for Nanomaterials, Bar-Ilan University, Ramat-Gan, 52900, Israel*

[4]*Moscow Steel and Alloys Institute, Leninskii Prospekt 4, Moscow 119049, Russia*

(Received 19 June 2008; revised manuscript received 23 July 2008; published 19 August 2008)

The size effect in electron-doped $La_{0.4}Ca_{0.6}MnO_3$ manganite compound was explored by dc magnetic and *X*-band electron magnetic resonance measurements in temperature intervals 5–350 K and 5–600 K. The analysis of experimental data verifies the stability of the antiferromagnetic ground state. It is suggested that the stability results from the localized nature of doped electrons in bulk and nanosamples, revealed by fitting the experimental electron paramagnetic resonance parameters to the theoretical models.

DOI: 10.1103/PhysRevB.78.052405 PACS number(s): 76.50.+g, 71.30.+h, 75.47.Lx

It is well known that finite-size effects induce a plethora of new phenomena in the solid-state magnetism.[1,2] In particular, it is believed that the reduction of a sample size down to the nanometer scale is capable of influencing the magnetic order in doped mixed valence manganites $R_{1-x}A_xMnO_3$ (R=La and rare earths, A=Ca, Sr, Ba, etc.) by changing the coupling between the spin subsystem (spins of both Mn ions and carriers) and the lattice. The point of special interest is the case of electron-doped manganites, or overdoped ones, with $x>0.5$. These materials are characterized usually by a stable antiferromagnetic (AFM) ground state and charge ordering (CO), i.e., the real-space order of Mn^{3+} and Mn^{4+} ions. Recently, experimental evidence of suppression of AFM/CO state in the $Pr_{0.5}Sr_{0.5}MnO_3$ and $Nd_{0.5}Ca_{0.5}MnO_3$ nanoparticles,[3,4] and $Pr_{0.5}Ca_{0.5}MnO_3$ nanowires,[5] i.e., in x=0.5 compounds on the border between hole- and electron-doped parts of the phase diagrams of respective manganite systems, were obtained.

More data are available for the prototypic $La_{1-x}Ca_xMnO_3$ (LCMO) system. It was reported[6] that LCMO (x=0.6) powders with mean grain size of 60 nm and 20 nm demonstrate ferromagnetic (FM)-like ordering with spontaneous magnetization $M_S \sim 1\ \mu_B$/f.u. at 5 K. The data by Zhang *et al.*[7] evidence that AFM/CO state continues to exist in LCMO (x=0.75) nanopowders, while the CO transition gradually shifts to lower temperatures and becomes broader with decreasing grain size. Note that the bulk LCMO (x=0.6) shows the CO transition at $T_{CO} \sim 260$ K, which is higher than the temperature $T_{CO} \sim 240$ K in the x=0.75 compound,[8] meaning that the CO state in the former case must be more stable. In addition, the results obtained for hole-doped (or underdoped) LCMO with x=0.1 and 0.3 show that x=0.1 nanopowders have notably different, FM-like, magnetic ground state than the bulk counterpart, characterized by mixed AFM+FM ground state.[9] At the same time, both nano- and bulk LCMO x=0.3 samples are FM ordered.[10] Thus, one may conclude that in LCMO system there is a clear tendency of weakening the size effect upon magnetic ordering, due to the ordering stabilization. In this context the data by Lu *et al.*[6] seem to be questionable. To obtain additional experimental insight into the problem we performed comparative dc magnetic and resonance studies on bulk and nano-LCMO (x=0.6) samples. We show that AFM/CO state is stable even in x=0.6 nanopowders with the grain size of 17 ± 2 nm, in agreement with the data of Ref. 7. The paramagnetic (PM) magnetic correlations and spin dynamics in nano- and bulk samples were probed by model fittings of electron PM resonance (EPR) parameters. As a result, a realistic model of the nanometer size effect on electron and magnetic order in $La_{0.4}Ca_{0.6}MnO_3$ compound is suggested. The revealed localized nature of doped electrons in the PM state of our samples seems to be a reason for the discussed stability of their AFM/CO ground state.

The LCMO (x=0.6) nanopowders with mean grain size of 17 ± 2 nm (determined by transmission electron microscopy and x-ray diffraction) were prepared by sonication-assisted coprecipitation[11] and subsequent crystallization at 900 K. The relatively small grain size enhances the size effects influence on the magnetic order. The bulk sample was synthesized in air atmosphere by a standard solid-state reaction at T=1350 °C. The crystallinity, composition, and stoichiometry of the nano- and bulk samples were tested by the x-ray diffraction (XRD), electron dispersive x-ray analysis and inductively coupled plasma atomic emission spectroscopy techniques, as described in Ref. 9. The room-temperature XRD spectra, showing the single phase nature of both samples, are presented in Fig. 1. On the basis of the Rietveld method,[12] the specimens were structurally described by the orthorhombic *Pnma* space group. Their lattice parameters are shown in Table I. The T- and magnetic field (H) dependences of dc magnetization M were measured using a superconducting quantum interference device (SQUID) magnetometer in the temperature range of 5–350 K and under H up to 5 T. The electron magnetic resonance (EMR), comprising EPR and ferromagnetic resonance, was measured with Bruker EMX-220 X-band (ν=9.4 GHz) spectrometer in the T-range 5–600 K using few milligrams of fine powdered samples, i.e., as-fabricated nanocrystals and/or the bulk ceramic, crushed up to micron-sized powder.[9] In the course of the experiments the T-dependences of the resonance field H_r,

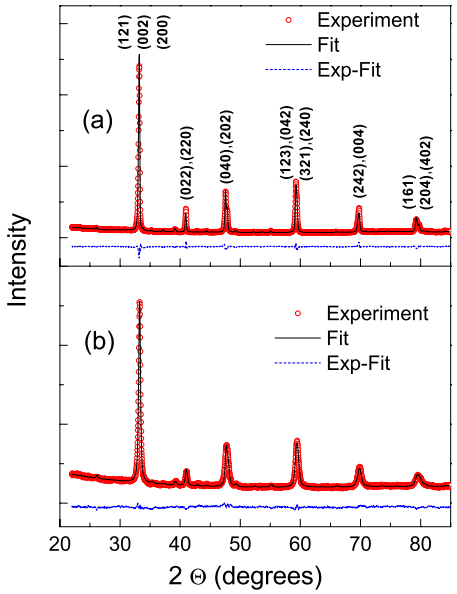

FIG. 1. (Color online) Observed (dots) and Rietveld fitted (lines) room-temperature x-ray diffraction patterns for (a) bulk (R_{wd}=4.6%) and (b) nanosized (R_{wd}=4.8%) $La_{0.4}Ca_{0.6}MnO_3$ samples.

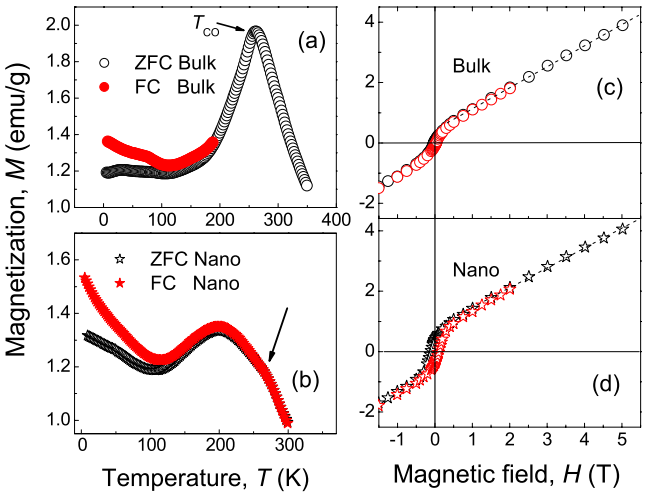

FIG. 2. (Color online) Temperature dependences of zero-field and field-cooled magnetizations measured at external field of 1 T on (a) bulk and (b) nanosized $La_{0.4}Ca_{0.6}MnO_3$; (c) and (d) hysteresis loops measured on the same samples at T=5 K. The arrow in (b) points out the "shoulder" of $M(T)$ curve. The dashed lines in (c) and (d) are the linear fits of the high-field $M(H)$ data for estimation of M_S values.

peak-to-peak linewidth ΔH_{pp}, and the doubly integrated intensity (DIN) of the EMR spectra were analyzed. The model fittings of the EPR signal DIN and ΔH_{pp} were carried out for both bulk and nanosamples.

Temperature dependence of dc magnetization measured at H=1 T after zero-field-cooling (ZFC) and field-cooling (FC) procedures are shown in Figs. 2(a) and 2(b) for bulk and nanosamples, respectively. The bulk $T_{CO}\sim 260$ K agrees well with the value reported in Refs. 6 and 8. However, in nanopowders a strong decrease in T_{CO} and broadening of the CO transition originated maximum, as compared to the bulk case, are observed. All these features, together with a "shoulder" at 260 K in $M(T)$ from Fig. 2(b), are consistent with the results by Zhang *et al.*[7] The values of T_{CO} and Néel temperature T_N, estimated using low-H $M(T)$ data, are shown in Table I. The FC and ZFC $M(T)$ curves of both nano and bulk split below $T\sim 150$ K, indicating that a low-T FM component coexists with a strong AFM one and its frustration is suppressed by a FC cycle. This finding confirms the coexistence of minor charge disordered FM and major CO AFM phases reported by Sagdeo *et al.*[13] for bulk LCMO with x =0.6, 0.67, and 0.7. Hysteresis loops recorded at T=5 K, see Figs. 2(c) and 2(d), evidence that $M_S\sim 0.045$ μ_B/f.u. of the nanopowder is about twice as large as in the bulk, in strong disagreement with the corresponding result by Lu *et al.*[6]

The EMR results shown in Fig. 3 are in fair agreement with our dc magnetic data. The EMR signal intensity (DIN) of the bulk shows a maximum at $T_{CO}\sim 260$ K, whereas a "shoulder" at the same temperature together with a maximum at $T\sim 185$ K appears in the nano case [see Fig. 3(a)]. These EMR data correlate with the critical temperatures revealed by $M(T)$ measurements (see Table I). Moreover, a sharp decrease in DIN upon cooling down to 5 K, usually attributed to the appearance of CO and AFM order at lower temperatures,[14] is observed in both nano and bulk. Neverthe-

TABLE I. Lattice parameters, temperatures of magnetic/electron transitions and the best-fit parameters for bulk and nanosamples of $La_{0.4}Ca_{0.6}MnO_3$ compound.

Sample	Bulk	Nano
a, b, c (Å), P_{nma} notation	5.395(1), 7.595(1), 5.402(1)	5.382(1), 7.573(1), 5.395(1)
$T_N(K)$	152 ± 2	152 ± 2
$T_{CO}(K)$	260 ± 2	198 ± 3
$\Theta(K)$ from DIN^{-1} fit	211 ± 5	213 ± 3, (401 ± 5)
$\Theta(K)$ from ΔH_{pp} fit	208 ± 2	205 ± 2
ΔH^{∞} (G) from ΔH_{pp} fit	2183 ± 17	2368 ± 18

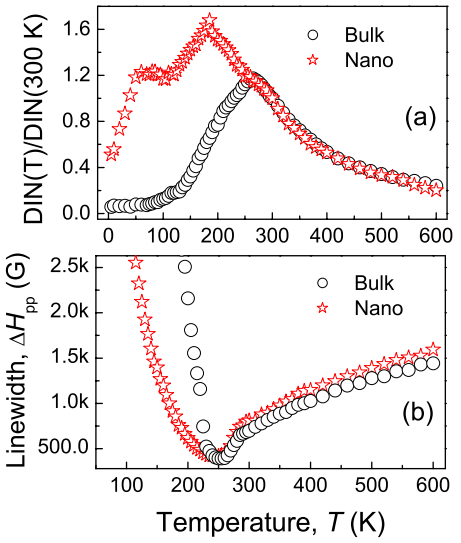

FIG. 3. (Color online) Temperature dependences of the EMR parameters: (a) normalized DIN and (b) linewidth for bulk and nanosized $La_{0.4}Ca_{0.6}MnO_3$.

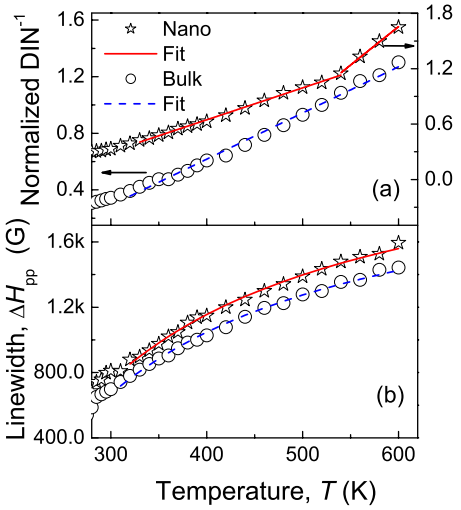

FIG. 4. (Color online) Temperature dependences of the EMR parameters: (a) normalized to its value at 300 K DIN^{-1} and (b) linewidth of EPR signals and their fits for bulk and nanosized $La_{0.4}Ca_{0.6}MnO_3$. The DIN$^{-1}(T)$ dependences in (a) are vertically shifted for clarity.

less, the decrease is less pronounced in the nano case confirming that the nanomagnetic ground state is characterized by the presence of a small, but stronger than in the bulk, FM component [see Figs. 2(c), 2(d), and 3(a)]. Note that DIN, being an EMR measure of the magnetic susceptibility, is sensitive mainly to static magnetic correlations, while the linewidth ΔH_{pp} probes the spin dynamics. The difference is evident in DIN (T) and $\Delta H_{pp}(T)$ curves in Fig. 3. It appears that $\Delta H_{pp}(T)$ dependences in both samples show pronounced minima near $T_{CO} \sim 260$ K. The sharp broadening of the EMR line below 260 K reflects the onset of CO state. The closeness of DIN in Fig. 3(a) and ΔH_{pp} in Fig. 3(b) in both samples at $T > T_{CO}$ should be noted.

It is argued in Ref. 9 that the DIN of Lorentzian EPR signal is proportional to thermodynamic susceptibility $(\chi_\perp)$ for a constant $H_r(T)$ and/or H-independent $\chi_\perp$ under the following assumption: $H_r(T) > \Delta H_{pp}(T)$. In our experiments the far PM EPR line was a single Lorentzian characterized by the same T-independent PM g-factor $g = 1.98 \pm 0.01$ (H_r =const) in nano- and bulk samples. Thus, we conclude that the proportionality DIN $\propto \chi_\perp$ is validated. The fair linearity of DIN^{-1} versus T in far PM range allows us to fit $\chi_\perp$ to the Curie-Weiss (CW) law, $\chi^{-1} \propto T - \Theta$, where Θ is CW temperature. The experimental data and their fit to the CW law are shown in Fig. 4(a). The only notable feature distinguishing nano- and bulk samples' behavior is the piecewise linearity of DIN$^{-1}(T)$ in the nano, with enhanced Θ at $T > 520$ K [see Fig. 4(a)]. We analyzed the $\Delta H_{pp}(T)$ dependences in Fig. 4(b) using Huber *et al.*'s[15] approach. Such an approach assumes strong exchange coupling providing bottleneck regime of resonating spins from atomic to nanometer scale. It appears[15] that

$$\Delta H_{pp}(T) = \frac{T - \Theta}{T} \Delta H^{\infty}, \tag{1}$$

where ΔH^{∞} is the high-T asymptote due to Mn ions spin-spin relaxation mechanism. Data in Fig. 4(b) show that Eq. (1) fits well the experimental $\Delta H_{pp}(T)$ in far PM range. The values of Θ and ΔH^{∞} obtained from the CW fits of DIN$^{-1}(T)$ and from the $\Delta H_{pp}(T)$ fits are also shown in Table I.

High concentration of doped electrons in $La_{0.4}Ca_{0.6}MnO_3$ compound results in the appearance of FM correlations in the PM state of both bulk and nanosamples as indicated by positive values of Θ in Table I. Moreover, Θ values obtained from different fitting procedures are very close, with the exception of Θ value for nano at high temperatures. This fact independently confirms the closeness of cation composition and oxygen stoichiometry of our samples since any stoichiometry difference must result in different Θ values due to the change in Mn^{3+} to Mn^{4+} ions' ratios. In general, the appearance of FM correlations in the PM state is a result of $Mn^{4+}-O-Mn^{3+}$ double exchange (DE) coupling. But contrary to the usual description of DE (Ref. 16) the coupling in LCMO $(x=0.6)$ seems to have a localized nature. In fact, it was shown[9] that when charge carriers in doped manganites can propagate in a bandlike manner, not only does long-range FM order emerge at low-T but PM spin relaxation of Mn ions is also drastically modified. Additional terms describing ion-electron spin-orbital and the electron spin-lattice interactions will appear then in Eq. (1). In our case, only the ion-ion mechanism fairly describes the PM spin relaxation in bulk and nanosamples. This confirms the minority nature of bandlike charge carriers in our samples and hence indicates the local nature of DE coupling.

Let us discuss briefly the electron and magnetic ordering in bulk and nanosamples upon cooling from the PM state. Between 600 K and 520 K the FM correlations (local DE coupling) in the nano are strongly different from the bulk ones as indicated by a twofold increase in CW temperature. The reason for this increase is still unknown. Upon approaching T_{CO} CO correlations between Mn^{4+} and Mn^{3+} ions begin to develop and to compete with the local FM ones. In the bulk such competition results in the appearance of long-

range CO below 260 K, while in the nano the temperature range of CO and FM correlations' coexistence expands down to $T \sim 200$ K. Only below 200 K, which is close to the values of PM Θ in Table I, the long-range CO becomes stable also in the nanocrystals. Since FM correlations are approximately of the same strength in both samples (see Table I), the latter result points to weaker CO correlations in the nanosample than in the bulk one. This explains, in principle, the low-T shift of the CO transition and broadening of the $M(T)$ maximum, associated with CO transition, upon decrease in the grain size in the nanosample, as reported in Ref. 7 and also observed in this work.

Let us emphasize that in both samples the low-T AFM/CO ground state appears due to the local nature of their DE interactions. This remains in a strong contrast to the hole-doped LCMO ($x=0.1$) case,[9] where the reduction in the grain size suppresses the chemical disorder, which results in a bandlike propagation of carriers and appearance of the FM-like ground state. We want to suggest that in LCMO ($x=0.6$) the localization of doped electrons is responsible for the type of magnetic ordering. This finding, as well as elastic interactions between Jahn-Teller ions,[17,18] may be considered as a prerequisite for the electron-hole doping asymmetry, i.e., FM and AFM ground states for equivalent levels of hole- and electron doping, in the LCMO phase diagram. The core-shell model of FM-like disordered shells on the background of AFM ordered cores[7] for electron-doped LCMO nanocrystals, together with intergrain interactions,[9] may explain the increase in the strength of the low-T FM component in the nanosamples. However, the nonsaturated $M(H)$ curves in Figs. 2(c) and 2(d), for applied fields up to 5 T, indicate the closeness of the values of differential susceptibility in both samples, and their similar strong AFM order which prevails at low temperatures.

Finally, it may be speculated that the nonstoichiometry of the sol-gel prepared nanosamples used by Lu *et al.*[6] is the reason for the observed FM-like ground state with $M_S \sim 1\ \mu_B$/f.u. This explanation is supported by data obtained by us with nanograined $La_{0.5}Ca_{0.5}MnO_3$ (not shown here), in which the decrease of the grain size down to ~ 30 nm really suppressed the unstable AFM/CO state, consistently with the results for other $x=0.5$ manganites.[3–5] The value of M_S was found to be close to 1 μ_B/f.u., which strongly confirms the nonstoichiometry induced shift of the effective level of Ca-doping in nanograined LCMO, studied in Ref. 6, to $x \sim 0.5$ value.

In summary, the experimental data and its analysis prove the enhanced stability of the AFM/CO ground state in $La_{0.4}Ca_{0.6}MnO_3$ compound with respect to the finite-size effects. It is suggested that the stability is increased due to the localized nature of doped electrons. The role of the localization as a prerequisite for electron-hole doping asymmetry in the $La_{1-x}Ca_xMnO_3$ phase diagram is currently being studied by us using other electron-doped compounds. It seems that the contradictory literature data concerning magnetic ordering in nano-$La_{0.4}Ca_{0.6}MnO_3$ may be explained by the extrinsic nonstoichiometry effects.

This research was supported by the Israeli Science Foundation administered by the Israel Academy of Sciences and Humanities (Grant No. 845/05). The authors thank G. Jung for fruitful discussions.

*Corresponding author; evgenyr@bgu.ac.il

[1] R. H. Kodama, J. Magn. Magn. Mater. **200**, 359 (1999).
[2] X. Batlle and A. Labarta, J. Phys. D **35**, R15 (2002).
[3] A. Biswas, I. Das, and Ch. Majumdar, J. Appl. Phys. **98**, 124310 (2005).
[4] S. S. Rao, S. Tripathi, D. Pandey, and S. V. Bhat, Phys. Rev. B **74**, 144416 (2006).
[5] S. S. Rao, K. N. Anuradha, S. Sarangi, and V. S. Bhat, Appl. Phys. Lett. **87**, 182503 (2005).
[6] C. L. Lu, S. Dong, K. F. Wang, F. Gao, P. L. Li, L. Y. Lv, and J.-M. Liu, Appl. Phys. Lett. **91**, 032502 (2007).
[7] T. Zhang, T. F. Zhou, T. Qian, and X. G. Li, Phys. Rev. B **76**, 174415 (2007).
[8] M. Pissas and G. Kallias, Phys. Rev. B **68**, 134414 (2003).
[9] E. Rozenberg, A. I. Shames, M. Auslender, G. Jung, I. Felner, J. Sinha, S. S. Banerjee, D. Mogilyansky, E. Sominski, A. Gedanken, Ya. M. Mukovskii, and G. Gorodetsky, Phys. Rev. B **76**, 214429 (2007).
[10] A. I. Shames, M. Auslender, E. Rozenberg, E. Sominski, A. Gedanken, and Ya. M. Mukovskii, J. Appl. Phys. **103**, 07F715 (2008).
[11] G. Pang, X. Xu, V. Markovich, S. Avivi, O. Palchik, Y. Koltypin, G. Gorodetsky, Y. Yeshurun, H. P. Buchkremer, and A. Gedanken, Mater. Res. Bull. **38**, 11 (2003).
[12] J. Rodriquez-Carvajal, Physica B (Amsterdam) **192**, 55 (1993).
[13] P. R. Sagdeo, Sh. Anwar, and N. P. Lalla, Phys. Rev. B **74**, 214118 (2006).
[14] A. I. Shames, E. Rozenberg, M. Auslender, G. Gorodetsky, C. Martin, A. Maignan, and Ya. M. Mukovskii, J. Magn. Magn. Mater. **290-291**, 910 (2005).
[15] D. L. Huber, G. Alejandro, A. Caneiro, M. T. Causa, F. Prado, M. Tovar, and S. B. Oseroff, Phys. Rev. B **60**, 12155 (1999).
[16] E. Dagotto, *Nanoscale Phase Separation and Colossal Magnetoresistance*, Springer Series in Solid State Physics Vol. 136 (Springer-Verlag, Berlin, 2003).
[17] D. Khomskii, Int. J. Mod. Phys. B **15**, 2665 (2001).
[18] D. I. Khomskii and K. I. Kugel, Phys. Rev. B **67**, 134401 (2003).